Afrika Matematika (2025) 36:115
https://doi.org/10.1007/s13370-025-01329-2

Discrete mode-mixtures of unimodal positive distributions with an application to solar energy in South Africa

A. Bekker[1] · A. F. Otto [1] · A. Punzo[2] · S. D. Tomarchio[2] · J. T. Ferreira[1,3]

Received: 18 December 2024 / Accepted: 18 May 2025

Abstract
Comprehensive earth science studies consistently yield complex datasets seldom adequately represented by straightforward parametric distributions. In this paper, we introduce a discrete mode-mixture (DMM) model, motivated by the formulation of the mean mixture paradigm via the compounding method. Here, unimodal positive support mode-parameterized beta and gamma distributions represent the basic component, but with the superposition of a discrete random component on the mode. The probability density functions of the DMM models are derived in closed-form expressions, and specific characteristics are investigated. This alternative viewing of a mixture on the mode paves the way for alternative models and provides natural leverage on separation in data. With an emphasis on a solar dataset and a benchmark dataset, the performance of the proposed models is compared with that of well-known models.

Keywords Beta · Compound · Gamma · Negative binomial · Poisson · SAURAN dataset · SDG 7 · SDG 13

1 Introduction

In light of the increased essential focus on clean and renewable energy, climate action—within the context of sustainable development goal 7 (affordable and clean energy) and 13 (climate action) [29]—and South Africa's dire power situation due to load shedding [45, 46], the consideration and analyses of solar energy production data is essential. The peculiarities of such data require innovative approaches for modeling—the modern-day statistician has experienced a staggering increase in the scale and scope of datasets, often with vastly different underlying characteristics, across all areas of scientific research. This highlights the necessity of flexible models encompassing significant heavy-tailedness and non-negligible skewness. Numerous approaches have been considered in the literature to deal with this challenge; for instance [19, 20, 25, 47].

✉ A. Bekker
andriette.bekker@up.ac.za

1 Department of Statistics, University of Pretoria, Pretoria, South Africa

2 Department of Economics and Business, University of Catania, Catania, Italy

3 School of Statistics and Actuarial Science, University of the Witwatersrand, Johannesburg, South Africa

Published online: 04 June 2025

The concept of location-scale mixtures originated several decades ago, as evidenced by the foundational works of [2, 49]. In short, it displays finite or continuous mixtures of reference (basic component) distributions concerning one or more of their parameters through a convenient discrete or continuous mixing distribution, with parameters that govern the overall model's flexibility; in the statistical literature, this approach is often called compounding. Compounding remains an intuitive theoretical approach to account for peculiarities present in data, and to describe them into a representative mathematical (and thus, statistical) framework [17, 18, 25]. According to [43], there are countless statistical models based on the location-scale mixture concept, but they can all be categorized according to how the compounding process is integrated into the model. Motivated by this, in this paper, we borrow the idea of mean mixtures [30], but from a mode viewpoint to construct a discrete mode-mixture (DMM) of positive support unimodal distributions. Multiple justifications exist for preferring the mode as a location parameter; refer to the discussion of [43] for further insights. As [9] points out, there is growing interest in evaluating numerous statistical models from a modal perspective. The mode, median, and mean are the three prevalent metrics of central tendency utilized in data analysis. However, for data originating from skewed distributions with large tails, the mode might be a more useful and intuitive indicator of central tendency [22] as the mode may be graphically located, is simply interpreted, and is unaffected by extremely high or low values.

This paper considers two 2-parameter mode-parametrized distributions as the reference distributions. First, we examine mode-parameterizations of the unimodal gamma and beta prime (beta type II) models, which are specified on positive support and parameterized by a mode parameter and a dispersion parameter.

Secondly, as discrete mixing distributions within the compound model, we consider the (a) Poisson, and (b) negative binomial, with parameters governing the tail weight. This is inspired by the weights usually considered in the shape mixture cases [6, 13, 14, 51]. The particular advantages, among others, for models constructed in this way is that i) for positive support data, we retain a clear and intuitive measure of central tendency (the mode), ii) there is no ambiguity on the modality of the models, and iii) the proposed mode-mixture construction is a previously unconsidered theoretical framework, but inspired from the well-known mean mixture methodology. We therefore extend and contribute to the literature with this unique perspective on positive support models indexed explicitly with a location type parameter. The resulting models have closed-form probability density functions (pdfs) and closed-form expressions for other statistical characteristics of interest, such as moments and moment generating functions.

Section 2 gives a brief background of the mode-parametrized gamma and beta prime distributions. By combining them as conditional distributions with the discrete models acting on the mode parameter, we introduce models within this mode-focused environment (Section 3). In Section 4, these flexible models are illustrated on solar irradiance data from South Africa (aligned with the focus on clean energy and climate action, as described earlier). In addition to this, these contributions to the literature are also fitted to the well-known Norwegian insurance dataset to benchmark our proposals. In both cases, our contributions are compared to other popular and often considered unimodal models with positive support [36, 37]. Section 5 summarizes the key aspects of this paper.

2 Background: 2-parameter mode-parameterized distributions

This section provides a brief overview of the gamma and the beta-prime distributions' mode parametrization and some of their properties. These will be the reference distributions in the compound models.

2.1 Mode-parameterized gamma distribution

Let X be a positive random variable having a gamma distribution with a pdf given by

$$f(x;\alpha,\beta)=\frac{1}{\Gamma(\alpha)\,\beta^{\alpha}}x^{\alpha-1}\exp(-x/\beta),\quad x>0, \tag{1}$$

where $\alpha>0$ and $\beta>0$ denote the shape and scale parameters, respectively, and $\Gamma(\cdot)$ denotes the usual gamma function. If $\alpha\geq 1$, the distribution is unimodal with the mode in $x=\beta(\alpha-1)$.

The pdf of the mode-parameterized gamma distribution that has been considered in [10], [4], and [37], is given by

$$f_{\mathrm{G}}(x;\theta,\gamma)=\frac{x^{\frac{\theta}{\gamma}}\exp\left(-\frac{x}{\gamma}\right)}{\Gamma\left(\frac{\theta}{\gamma}+1\right)\gamma^{\frac{\theta}{\gamma}+1}},\quad x>0, \tag{2}$$

where $\theta>0$ is the mode and $\gamma>0$ is a dispersion parameter. Figure 1a illustrates the impact of varying γ (when $\theta=2$), and Figure 1b illustrates the impact of varying θ (when $\gamma=0.5$). See [4] for further details on how these parameters affect the distribution's shape. The link between the parameterizations (1) and (2) is given by

$$\begin{cases}\alpha=\frac{\theta}{\gamma}+1\\ \beta=\gamma\end{cases}\quad\Longrightarrow\quad\begin{cases}\theta=\beta(\alpha-1)\\ \gamma=\beta\end{cases}.$$

The s^{th} moment for a variable with pdf (2) is given by

$$\mathrm{E}\left(X^{s}\right)=\frac{\Gamma\left(\frac{\theta}{\gamma}+s+1\right)\gamma^{s}}{\Gamma\left(\frac{\theta}{\gamma}+1\right)}.$$

Specifically, the variance is $\gamma^2+\theta\gamma$, while the moment-generating function (mgf) has the form

$$M_X(t)=\frac{1}{(1-\gamma t)^{\frac{\theta}{\gamma}+1}}.$$

2.2 Mode-parameterized beta prime distribution

The pdf of the beta prime (BP) distribution [11] is given by

$$f(x;\alpha,\beta)=\frac{x^{\alpha-1}(1+x)^{-(\alpha+\beta)}}{B(\alpha;\beta)},\quad x>0, \tag{3}$$

where $\alpha>0$ and $\beta>0$ are two shape parameters, and $B(\cdot,\cdot)$ denotes the usual beta function. It is known that if $\alpha\geq 1$, the pdf in (3) will have a single mode at $x=\frac{\alpha-1}{\beta+1}$.

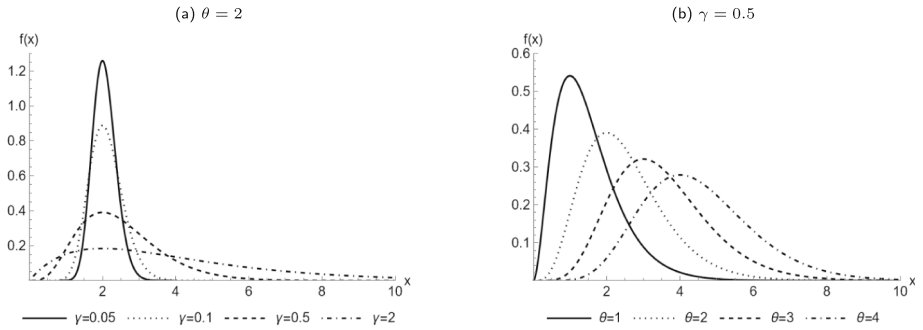

Fig. 1 Mode-parameterized gamma (2) with $\theta = 2$ (left panel) and $\gamma = 0.5$ (right panel)

We introduce the mode-parameterized beta prime distribution with pdf

$$f_{\text{BP}}(x;\theta,\gamma) = \frac{x^{\left(3+\frac{1}{\gamma}\right)\theta}(1+x)^{-\frac{(1+3\gamma)(1+\theta)}{\gamma}}}{B\left(1+\left(3+\frac{1}{\gamma}\right)\theta;2+\frac{1}{\gamma}\right)}, \quad x>0, \tag{4}$$

where $\theta > 0$ is the mode and $\gamma > 0$ is a dispersion parameter, similar to the unimodal gamma distribution defined in (2). The link between the parameterizations (3) and (4) is

$$\begin{cases} \alpha = 1+\left(3+\frac{1}{\gamma}\right)\theta \\ \beta = 2+\frac{1}{\gamma} \end{cases} \implies \begin{cases} \theta = \frac{\alpha-1}{\beta+1} \\ \gamma = \frac{1}{\beta-2}. \end{cases}$$

The s^{th} moment for a variable with the pdf in (4) is given by

$$\text{E}\left(X^s\right) = \frac{\Gamma\left(\left(3+\frac{1}{\gamma}\right)\theta+s+1\right)\Gamma\left(2+\frac{1}{\gamma}-s\right)}{\Gamma\left(\left(3+\frac{1}{\gamma}\right)\theta+1\right)\Gamma\left(2+\frac{1}{\gamma}\right)},$$

where the mean and variance are

$$\text{E}(X) = \frac{(3\gamma+1)\theta+\gamma}{1+\gamma}$$

and

$$\text{Var}(X) = \frac{\gamma(\gamma+\theta+3\gamma\theta)(1+\theta+\gamma(2+3\theta))}{(\gamma+1)^2}.$$

The mgf for (4) is given by

$$M_X(t) = \exp(-t)\frac{\Gamma\left[3+\left(3+\frac{1}{\gamma}\right)\theta+\frac{1}{\gamma}\right]}{\Gamma\left[2+\frac{1}{\gamma}\right]}G^{2,0}_{1,2}\left[-t\Big|_{2+\frac{1}{\gamma},0}^{3+\left(3+\frac{1}{\gamma}\right)\theta+\frac{1}{\gamma}}\right],$$

where $G(\cdot)$ is Meijer's G-function [24].

Analogous to the gamma pdf (2) (see [4]), Figure 2 illustrates how the beta prime pdf shape changes for $\theta = 2$ (left panel) and $\gamma = 0.5$ (right panel).

We restrict our attention to the subclass of unimodal, hump-shaped pdfs for both the gamma and beta-prime distributions, excluding all reverse J-shaped cases that exhibit an asymptote at $x = 0$.

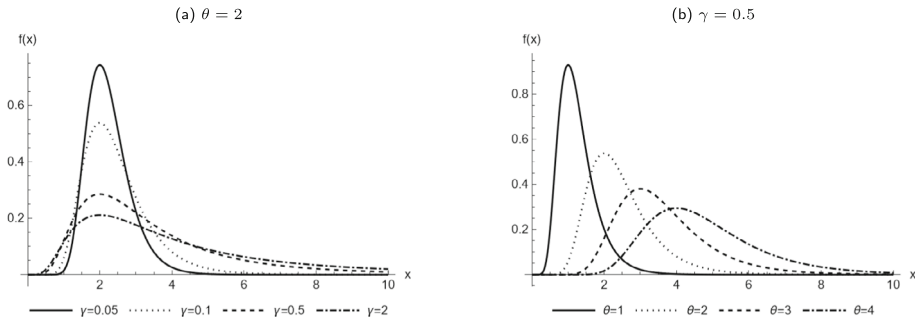

Fig. 2 Mode-parameterized beta prime (4) with $\theta = 2$ (left panel) and $\gamma = 0.5$ (right panel)

3 General framework for DMM of positive support unimodal distributions

We propose a compound approach inspired by the normal mean mixture, where the mode parameter, θ, from (2) and (4), is shifted to the right by a positive mixing variable. This mixing variable has a probability density or mass function h, which is characterized by a (potentially vector) shape parameter $\boldsymbol{\phi}$. The selected mixing distributions offer the advantage of yielding a compound model with a closed-form pdf, a feature of significant importance [41]. In particular, we focus on discrete mixing variables.

In Definitions 1 and 2, we introduce the DMM of positive support unimodal distributions, with a focus on the mode-parameterized gamma and mode-parameterized beta prime as the (conditional) unimodal distributions. The *mixing distribution* we will implement is discrete – led by the noncentral representations of many models that are effectively shape mixtures based on Poisson weights [6, 14, 34, 51].

Definition 1 (Gamma DMM) A positive random variable X is said to have the DMM of gamma distributions with mode $\theta > 0$, dispersion parameter $\gamma > 0$, and (potentially vector) shape parameter $\boldsymbol{\phi}$, if the pdf is given by

$$p(x; \theta, \gamma, \boldsymbol{\phi}) = \sum_{j=0}^{\infty} f_{\mathrm{G}}(x; \theta + j\gamma, \gamma) h(j; \boldsymbol{\phi}), \quad x > 0, \tag{5}$$

where f_{G} is the unimodal conditional gamma pdf in (2), and $h(j; \boldsymbol{\phi})$ is a mixing probability mass function (pmf) indexed by the vector of parameters $\boldsymbol{\phi}$.

Definition 2 (Beta prime DMM) A positive random variable X is said to have the DMM of beta prime distributions with mode $\theta > 0$, dispersion parameter $\gamma > 0$, and (potentially vector) shape parameter $\boldsymbol{\phi}$, if the pdf is given by

$$p(x; \theta, \gamma, \boldsymbol{\phi}) = \sum_{j=0}^{\infty} f_{\mathrm{BP}}(x; (3\gamma + 1)\theta + j\gamma, \gamma) h(j; \boldsymbol{\phi}), \quad x > 0, \tag{6}$$

where f_{BP} is the unimodal conditional beta prime pdf in (4) and $h(j; \boldsymbol{\phi})$ is a pmf indexed by the vector of parameters $\boldsymbol{\phi}$.

The distribution of X can be considered a composite distribution constructed by taking an infinite set of component distributions by adding an index j to the mode scaled by the variability parameter. We consider two mixing distributions: Poisson and negative binomial. The

Poisson distribution we consider, compactly denoted as Pois($\frac{\lambda}{2}$), depends on the parameter $\frac{\lambda}{2}$, and has pmf

$$h_{\mathrm{P}}(j;\lambda)=\frac{\exp\left(-\frac{\lambda}{2}\right)\left(\frac{\lambda}{2}\right)^{j}}{j!},\quad j=0,1,2,\ldots \text{ and } \lambda>0. \tag{7}$$

As the second choice for a mixing distribution, we consider the negative binomial distribution with parameters r and p, compactly denoted as NB(r, p). If $r=1$, the geometric distribution follows. This distribution is implemented to model count data and overcomes the equidispersion constraint of the Poisson distribution. The pmf is given by

$$h_{\mathrm{NB}}(j;r,p)=\binom{j+r-1}{j}p^{r}(1-p)^{j},\quad j=0,1,2,\ldots,\ \text{for}\ r>0\ \text{and}\ 0\leq p\leq 1. \tag{8}$$

Both (5) and (6) will be unimodal hump-shaped (see Appendix). As we have mentioned before, the conditional distribution f in (5) and (6) is embedded as a special case of either (5) or (6) if $\lambda\to 0$, for the Poisson mixing variable, and $p\to 1$ for the negative binomial mixing variable.

The alert reader will notice the difference between the proposed compound models and models in literature that are being referred to as compound gamma, compound gamma-Poisson, Poisson compound gamma, Poisson beta, beta negative binomial; see for example [15, 21, 28, 32, 35, 48, 50].

3.1 Poisson mixing distribution

3.1.1 Conditional gamma distribution

Using (7) in model (5), we obtain the following pdf for the mode Gamma-Poisson (G-P)

$$\begin{aligned}p_{\text{G-P}}(x;\theta,\gamma,\lambda)&=\sum_{j=0}^{\infty}\frac{x^{\frac{\theta}{\gamma}+j}\exp(-\frac{x}{\gamma})}{\Gamma\left(\frac{\theta}{\gamma}+j+1\right)\gamma^{\frac{\theta}{\gamma}+j+1}}\frac{\exp\left(-\frac{\lambda}{2}\right)\left(\frac{\lambda}{2}\right)^{j}}{j!}\\&=\frac{x^{\frac{\theta}{\gamma}}\exp(-\frac{x}{\gamma})}{\Gamma\left(\frac{\theta}{\gamma}+1\right)\gamma^{\frac{\theta}{\gamma}+1}\exp\left(\frac{\lambda}{2}\right)}\,{}_0F_1\left(\frac{\theta}{\gamma}+1;\frac{x\lambda}{2\gamma}\right),\quad x>0,\end{aligned} \tag{9}$$

with $\theta,\gamma,\lambda>0$ and ${}_0F_1(\cdot)$ being a hypergeometric function with scalar argument. Using [16] p. 815, eq. (9), the mgf becomes

$$\begin{aligned}M_X(t)&=\frac{x^{\frac{\theta}{\gamma}}\exp(-\frac{x}{\gamma})}{\Gamma\left(\frac{\theta}{\gamma}+1\right)\gamma^{\frac{\theta}{\gamma}+1}\exp\left(\frac{\lambda}{2}\right)}\int_0^{\infty}\exp\left(-x\left(\frac{1}{\gamma}-t\right)\right)x^{\frac{\theta}{\gamma}}\,{}_0F_1\left(\frac{\theta}{\gamma}+1;\frac{x\lambda}{2\gamma}\right)dx\\&=\frac{\exp\left(\frac{\lambda}{2\gamma(1-\gamma t)}\right)}{(1-\gamma t)^{\frac{\theta}{\gamma}+1}}.\end{aligned}$$

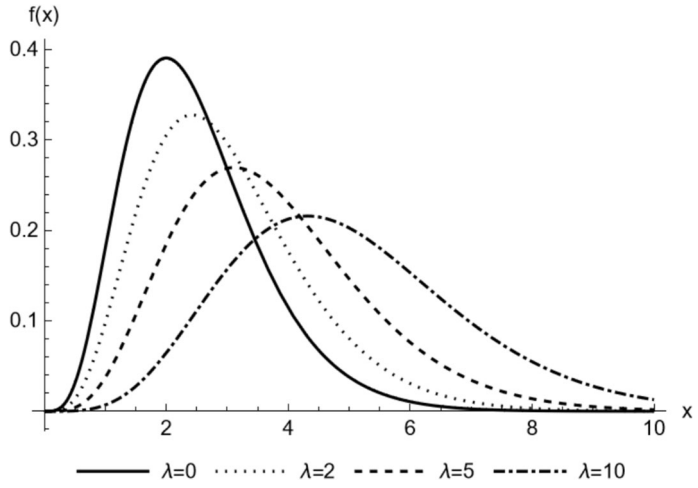

Fig. 3 Mode G-P mixture (9)

Similarly, the s^{th} moment is given by

$$\mathrm{E}\left(X^s\right) = \frac{\Gamma\left(\frac{\theta}{\gamma}+s+1\right)\gamma^s}{\Gamma\left(\frac{\theta}{\gamma}+1\right)\exp\left(\frac{\lambda}{2}\right)}\,{}_1F_1\left(\frac{\theta}{\gamma}+s+1;\frac{\theta}{\gamma}+1;\frac{\lambda}{2}\right), \tag{10}$$

where ${}_1F_1(\cdot)$ is the confluent hypergeometric function with scalar argument. Using (10), the variance can be calculated easily, using $\mathrm{Var}(X) = \mathrm{E}(X^2) - [\mathrm{E}(X)]^2$.

Importantly, this model (as well as subsequent ones) has one unique mode – in the case of (9), it is given by

$$m_{\text{G-P}} = \theta + \gamma\frac{\Gamma\left(\frac{\theta}{\gamma}+1\right)}{{}_0F_1\left(\frac{\theta}{\gamma}+1;\frac{\lambda}{2\gamma}\right)}\sum_{j=1}^{\infty}\frac{\left(\frac{\lambda}{2\gamma}\right)^j}{\Gamma(j)\,\Gamma\left(\frac{\theta}{\gamma}+j+1\right)},$$

where the proof is outlined in the Appendix. If $\lambda \to 0$, the mode reduces to θ, which conveniently is the mode of the reference (conditional) model. It is also valuable to note that for any increasing value of λ, the value of $m_{\text{G-P}}$ will also increase. Similar observations are made for all subsequent models in this paper.

For the reader's interest, the effect of varying λ, with fixed $\theta = 2$ and $\gamma = 0.5$, is illustrated in Figure 3.

3.1.2 Conditional beta prime distribution

Using (7) in (4), we obtain the mode BP-Poisson (BP-P) distribution with pdf

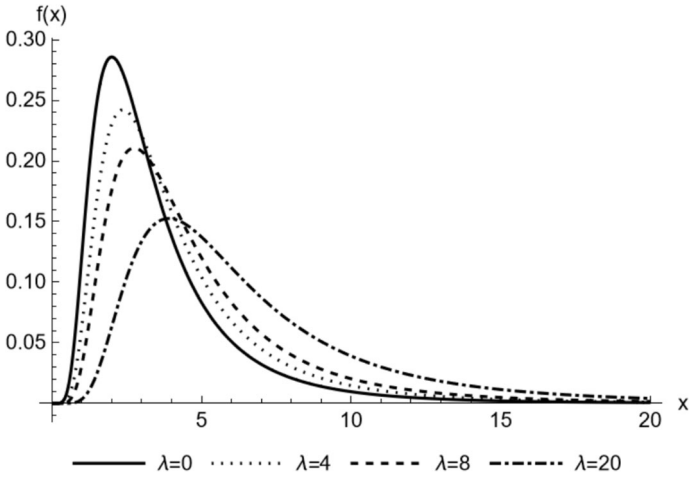

Fig. 4 Mode BP-P mixture (11)

$$
\begin{aligned}
p_{\text{BP-P}}(x;\theta,\gamma,\lambda) &= \sum_{j=0}^{\infty} \frac{x^{\left(3+\frac{1}{\gamma}\right)\theta+j}\,(1+x)^{-\left(\frac{1+3\gamma}{\gamma}+\frac{1+3\gamma}{\gamma}\theta+j\right)}}{B\left(1+\left(3+\frac{1}{\gamma}\right)\theta+j;2+\frac{1}{\gamma}\right)} \frac{\exp\left(-\frac{\lambda}{2}\right)\left(\frac{\lambda}{2}\right)^{j}}{j!} \\
&= \frac{x^{\left(3+\frac{1}{\gamma}\right)\theta}\,(1+x)^{-\left(\frac{1+3\gamma}{\gamma}+\frac{1+3\gamma}{\gamma}\theta\right)}}{\exp\left(\frac{\lambda}{2}\right)B\left(1+\left(3+\frac{1}{\gamma}\right)\theta;2+\frac{1}{\gamma}\right)}\,{}_1F_1 \\
&\quad \left(3+\left(3+\frac{1}{\gamma}\right)\theta+\frac{1}{\gamma},1+\left(3+\frac{1}{\gamma}\right)\theta;\frac{\lambda x}{2(1+x)}\right), \\
&\quad x>0, \qquad (11)
\end{aligned}
$$

with $\theta, \gamma, \lambda > 0$. Using [12], p. 338, an expression for the s^{th} moment is given by

$$
\mathrm{E}\left(X^s\right) = \frac{\Gamma\left(\frac{1+3\gamma}{\gamma}-s-1\right) G_{2,3}^{1,2}\left[\frac{\lambda}{2}\Big|_{0,-\left(3+\frac{1}{\gamma}\right)\theta,1-\left(\frac{1+3\gamma}{\gamma}+\left(\frac{1+3\gamma}{\gamma}\right)\theta\right)}^{-\left[\left(3+\frac{1}{\gamma}\right)\theta+s\right],-\left[\left(3+\frac{1}{\gamma}\right)\theta+2+\frac{1}{\gamma}\right]}\right]}{\exp\left(\frac{\lambda}{2}\right)\Gamma\left(2+\frac{1}{\gamma}\right)}, \qquad (12)
$$

for $s < 2+\frac{1}{\gamma}$. As before, one can use (12), to calculate the variance of X, using $\mathrm{Var}(X) = \mathrm{E}(X^2) - [\mathrm{E}(X)]^2$. The single mode of this model ($m_{\text{BP-P}}$) is given by

$$
m_{\text{BP-P}} = \theta + \gamma \frac{\sum_{j=1}^{\infty} \frac{\left(\frac{\lambda}{2}\right)^j \left(3+\left(3+\frac{1}{\gamma}\right)\theta+\frac{1}{\gamma}\right)_j}{\Gamma(j)\left(1+\left(3+\frac{1}{\gamma}\right)\theta\right)_j}}{(1+3\gamma)_1 F_1\left(3+\left(3+\frac{1}{\gamma}\right)\theta+\frac{1}{\gamma};1+\left(3+\frac{1}{\gamma}\right)\theta;\frac{\lambda}{2}\right)}.
$$

Figure 4 describes the behavior of the pdf in (11) for varying λ, with $\theta = 2$ and $\gamma = 0.5$.

3.2 Negative binomial mixing variable

3.2.1 Conditional gamma distribution

From (5) and (8) the pdf of the mode Gamma-Negative Binomial (G-NB) is given by the closed form expression:

$$p_{\text{G-NB}}(x;\theta,\gamma,r,p) = \sum_{j=0}^{\infty} \frac{x^{\frac{\theta}{\gamma}+j}\exp(-\frac{x}{\gamma})}{\Gamma\left(\frac{\theta}{\gamma}+j+1\right)\gamma^{\frac{\theta}{\gamma}+j+1}}\binom{j+r-1}{r-1}p^r(1-p)^j$$
$$= \frac{x^{\frac{\theta}{\gamma}}\exp(-\frac{x}{\gamma})p^r}{\Gamma\left(\frac{\theta}{\gamma}+1\right)\gamma^{\frac{\theta}{\gamma}+1}}\,{}_1F_1\left(r;\frac{\theta}{\gamma}+1;\frac{x(1-p)}{\gamma}\right),\ x>0, \quad (13)$$

where $\theta,\gamma,r>0$ and $0\le p\le 1$. Using [16], p. 815, eq. (9), with the mgf beocmes

$$M_X(t) = \frac{p^r}{\Gamma\left(\frac{\theta}{\gamma}+1\right)\gamma^{\frac{\theta}{\gamma}+1}}\int_0^{\infty}\exp\left(-x\left(\frac{1}{\gamma}-t\right)\right)x^{\frac{\theta}{\gamma}}\,{}_1F_1\left(r;\frac{\theta}{\gamma}+1;\frac{x(1-p)}{\gamma}\right)dx$$
$$= \left(\frac{p(1-t\gamma)}{p-\gamma t}\right)^r\frac{1}{(1-\gamma t)^{\frac{\theta}{\gamma}+1}}.$$

Similarly the s^{th} moment is given by

$$\mathrm{E}\left(X^s\right) = \frac{\Gamma\left(\frac{\theta}{\gamma}+s+1\right)(p\gamma)^s}{\Gamma\left(\frac{\theta}{\gamma}+1\right)}\,{}_2F_1\left(r,\frac{\theta}{\gamma}+s+1;\frac{\theta}{\gamma}+1;\frac{(1-p)}{\gamma}\right),$$

where ${}_2F_1(\cdot)$ is the Gauss hypergeometric function with scalar argument $\left|\frac{1-p}{\gamma}\right|<1$. The mode of the G-NB ($m_{\text{G-NB}}$) is given by

$$m_{\text{G-NB}} = \theta+\gamma\frac{\Gamma\left(\frac{\theta}{\gamma}+1\right)}{{}_1F_1\left(r;\frac{\theta}{\gamma}+1;\frac{1-p}{\gamma}\right)}\sum_{j=1}^{\infty}\frac{(r)_j\left(\frac{1-p}{\gamma}\right)^j}{\Gamma(j)\,\Gamma\left(\frac{\theta}{\gamma}+j+1\right)}.$$

The effect of varying r and p for $\theta=2$ and $\gamma=0.5$, by a set of G-NB pdfs, is displayed in Figure 5.

3.2.2 Conditional beta prime distribution

Using (8) in (4), we obtain the mode BP-NB distribution with pdf

$$p_{\text{BP-NB}}(x;\theta,\gamma,r,p)$$
$$= \sum_{j=0}^{\infty}\frac{x^{\left(3+\frac{1}{\gamma}\right)\theta+j}(1+x)^{-\left(\frac{1+3\gamma}{\gamma}+\frac{1+3\gamma}{\gamma}\theta+j\right)}}{B\left(1+\left(3+\frac{1}{\gamma}\right)\theta+j;2+\frac{1}{\gamma}\right)}\binom{j+r-1}{r-1}p^r(1-p)^j$$
$$= \frac{x^{\left(3+\frac{1}{\gamma}\right)\theta}(1+x)^{-\left(\frac{1+3\gamma}{\gamma}+\frac{1+3\gamma}{\gamma}\theta\right)}p^r}{B\left(1+\left(3+\frac{1}{\gamma}\right)\theta;2+\frac{1}{\gamma}\right)}$$

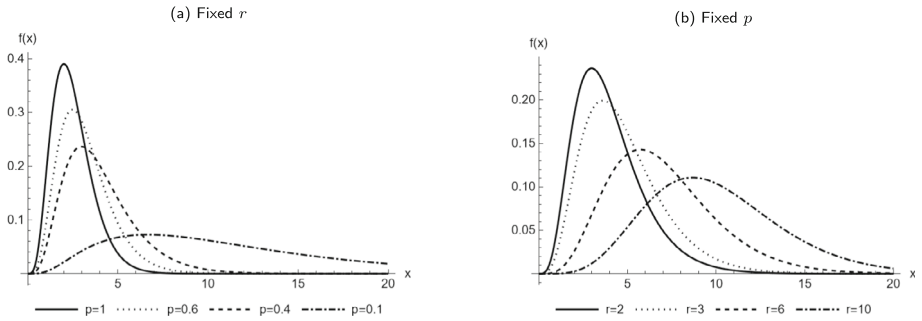

Fig. 5 Mode G-NB (13) for fixed r (left panel) and fixed p (right panel)

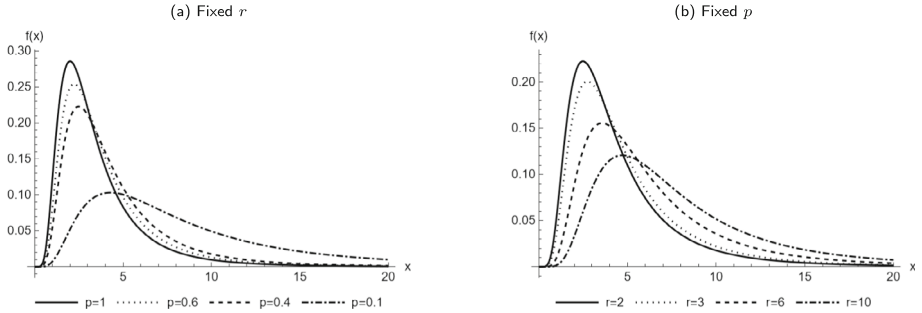

Fig. 6 Mode BP-NB ((14) for fixed r (left panel) and fixed p (right panel)

$$ {}_2F_1\left(r, 3+\left(3+\frac{1}{\gamma}\right)\theta+\frac{1}{\gamma}, 1+\left(3+\frac{1}{\gamma}\right)\theta; \frac{x(1-p)}{(1+x)}\right), \quad \text{x>0}, \tag{14} $$

where $\theta > 0, \gamma > 0, r > 0$ and $0 \leq p \leq 1$. An expression for the s^{th} moment is given by

$$ E\left(X^s\right) = \frac{p^r \Gamma(3+\frac{1}{\gamma}-s-1)}{\Gamma\left(2+\frac{1}{\gamma}\right)} \sum_{k=0}^{\infty} \frac{(r)_k\,(1-p)^k \Gamma\left(\left(3+\frac{1}{\gamma}\right)\theta+s+k+1\right)}{k!\Gamma(1+\left(3+\frac{1}{\gamma}\right)\theta+k)}, $$

for $s < 2+\frac{1}{\gamma}$. The mode of the BP-NB ($m_{\text{BP-NB}}$) is given by

$$ m_{\text{B-NB}} = \theta + \gamma \frac{\sum_{j=1}^{\infty} \frac{(r)_j (1-p)^j \left(3+\left(3+\frac{1}{\gamma}\right)\theta+\frac{1}{\gamma}\right)_j}{\Gamma(j)\left(1+\left(2+\frac{1}{\gamma}\right)\theta\right)_j}}{(1+3\gamma)_1\, F_1\left(3+\left(3+\frac{1}{\gamma}\right)\theta+\frac{1}{\gamma}; 1+\left(3+\frac{1}{\gamma}\right)\theta; 1-p\right)}. $$

Figure 6 describes the behaviour of the pdf in (14) for varying r (fixed $p = 0.5$) and p (fixed $r = 2$) with $\theta = 2$ and $\gamma = 0.5$.

Advantageously, these DMM models guarantee unimodality in X for our specific choices of mixing distributions (see Appendix). This construction allows that the conditional distributions (basic components) are special cases of the proposed models when $\lambda \to 0$, for the Poisson mixing or $p \to 1$ for the negative binomial mixing, this results in nested models.

3.3 Parameter estimation via maximum likelihood

Maximum likelihood (ML) is employed to obtain estimates of the parameters for the proposed DMM of positive support unimodal distributions. Given a random sample $x_1, \ldots, x_n$ from either pdfs (5) and (6), the log-likelihood function is given by

$$l(\theta, \gamma, \boldsymbol{\phi}) = \sum_{i=1}^{n} \ln \left[p(x_i; \theta, \gamma, \boldsymbol{\phi}) \right]. \tag{15}$$

The first order partial derivatives of (15), with respect to $(\theta, \gamma, \boldsymbol{\phi}')'$, are

$$l'(\theta, \gamma, \boldsymbol{\phi}) = \sum_{i=1}^{n} \frac{\partial}{\partial(\theta, \gamma, \boldsymbol{\phi})} \ln \left[p(x_i; \theta, \gamma, \boldsymbol{\phi}) \right]. \tag{16}$$

The values of θ, γ and $\boldsymbol{\phi}$ that maximize $l(\theta, \gamma, \boldsymbol{\phi})$ are the ML estimates $\widehat{\theta}$, $\widehat{\gamma}$, and $\widehat{\boldsymbol{\phi}}$ and satisfy the condition $l'(\widehat{\theta}, \widehat{\gamma}, \widehat{\boldsymbol{\phi}}) = \mathbf{0}$. Numerical methods may be employed to maximize the log-likelihood function in cases when closed-form estimates are not readily available, subject to constraints that may be present on the parameters.

4 Data application

The real data analyses are conducted in `R`; the codes are available upon request. We perform maximization of (15) numerically by the general-purpose numerical optimizer `optim()` for `R` [39]. Both the Nelder-Mead and the BFGS algorithms were used. Ultimately, the solution providing the best-observed data log-likelihood value was retained (see [42]). These algorithms are used in conjunction with the following transformations/back-transformations:

$$\begin{array}{rcl}
\widetilde{\theta} = \ln \theta & \leftrightarrow & \theta = \exp(\widetilde{\theta}) \\
\widetilde{\gamma} = \ln \gamma & \leftrightarrow & \gamma = \exp(\widetilde{\gamma}) \\
\widetilde{\lambda} = \ln \lambda & \leftrightarrow & \lambda = \exp(\widetilde{\lambda}) \\
\widetilde{p} = \ln(\frac{p}{1-p}) & \leftrightarrow & p = \exp(\widetilde{p})/\left(\exp(\widetilde{p}) + 1\right) \\
\widetilde{r} = \ln r & \leftrightarrow & r = \exp(\widetilde{r})
\end{array}$$

to account for the parameter constraints.

For the hypergeometric functions, the `hypergeo` package is used. The empirical mode of the dataset is used as an initial parameter for θ for both the gamma and beta prime distributions. The empirical mode is determined as the value with the highest density based on the kernel density estimator provided by the `density()` function from `R`'s `stats` package, using its default arguments [31, 36–38]. The initial estimates of γ are obtained by ML-fitting of the conditional gamma and negative binomial distributions. The initial values of $\boldsymbol{\phi}$ are such that the proposed models tend to the respective conditional models.

4.1 Real data analyses

The performance of the proposed models is compared to alternative models by considering a new dataset relevant to climate modeling (Section 4.1.1), followed by a widely known dataset (Section 4.1.2). To compare models in terms of goodness-of-fit with the same number of parameters, the log-likelihood is considered; when the number of parameters differs, we

use the Akaike information criterion (AIC; [1]) and the Bayesian information criterion (BIC; [40]).

4.1.1 Surface solar irradiance

Solar irradiance variation significantly impacts the performance of instantaneous non-linear devices such as solar energy converters [3]. Therefore, by quantifying the solar irradiance variability, effective management of power systems that inject solar-generated power into the energy grid is possible [27]. Furthermore, this can lead to improving these power systems to potentially avoid costly grid reinforcements, [26], resulting from voltage and frequency fluctuations and instabilities [23]. Several components contribute to solar irradiance depletion before it reaches the Earth's surface, such as aerosols, ozone molecules, and clouds, with clouds being the main component. We are interested in "statistical solar climatology," which is used to achieve instantaneous solar energy conversion goals [44]. This comprises statistical data analysis on the main variables of interest, such as direct normal irradiance (DNI), diffused horizontal irradiance (DHI), and global horizontal irradiance (GHI) of specific locations at specific times. The interested reader is referred to [33].

South Africa has great potential for solar energy production as it has sunshine all year round, with an average of more than 2500 hours of sunlight per year and an average solar radiation level of between 4.5-6.5 kilowatt-hour per square meter (kWh/m^2) per day. For this paper, we are interested in modeling the diffused irradiance index. This is normalized to eliminate the deterministic variation and time dependency within the irradiance variables resulting from the sun's movement in the sky throughout each day. To the authors' knowledge, only the gamma distribution is applied for the unimodal behavior of this variable in the literature [26].

In this paper, the minute-average solar irradiance data for 1 January 2021 until 31 December 2021 (which includes the GHI, DHI, and DNI values) are obtained from the Southern Africa Universities Radiometric Network (SAURAN) database for two locations in South Africa. The two radiometric stations are situated at the (a) University of Pretoria (UP) (latitude: -25.75308037, longitude: 28.22859001) in Gauteng and at (b) Stellenbosch University (SUN) (latitude: -33.92810059, longitude: 18.86540031) in the Western Cape. Kipp and Zonen CMP11 pyranometers were used to capture the data for the GHI and DHI variables, whereas SOLYS-2 trackers and CHP1 pyrheliometers were used to capture the data for the DNI variable. It is worth noting that the pyranometers at SUN and UP were last calibrated on 2016/09/06 and 2018/08/11, respectively.

For this paper, we only considered the solar irradiance during the daylight hours in the presence of sunlight. To mitigate the removal of observations, we have chosen the following margins for both of the locations: for the UP dataset, a margin of between 7:00 and 17:00 was chosen since the latest the sun came up was on 2 July 2021 at 6:54, and the earliest it went down was on 9 June 2021 at 17:23. For the SUN dataset, a margin of between 8:00-17:00 was chosen since the latest the sun came up was on 30 June 2021 at 7:50 and the earliest it went down was on 12 June 2021 at 17:42. The descriptive statistics are given in Table 1. It is observed that the minute average has a positive skewness and excess kurtosis.

We compared the proposed models with the following compound models by [37]: (a) G-G (unimodal gamma for both conditional and mixing distribution), (b) LN-LN (lognormal for both conditional and mixing distribution), and (c) IG-IG (inverse Gaussian for both conditional and mixing distributions). Figures 7 and 8 illustrate the fitted pdfs superimposed on the diffused irradiance index data for UP and SUN, respectively. Tables 2 and 3 show the performance measures for the considered models. From the results in these tables, the AIC

Table 1 Descriptive statistics of minute-average data for GHI(W/m^2)

	Min	Q1	Median	Mean	Q3	Max	Skewness	Kurtosis
UP	0.1174	251.4175	487.9658	509.3179	724.3266	1553.2980	0.3267	2.2181
SUN	0.7761	277.3994	528.6825	535.2764	780.1922	2367.2900	0.1325	2.0559

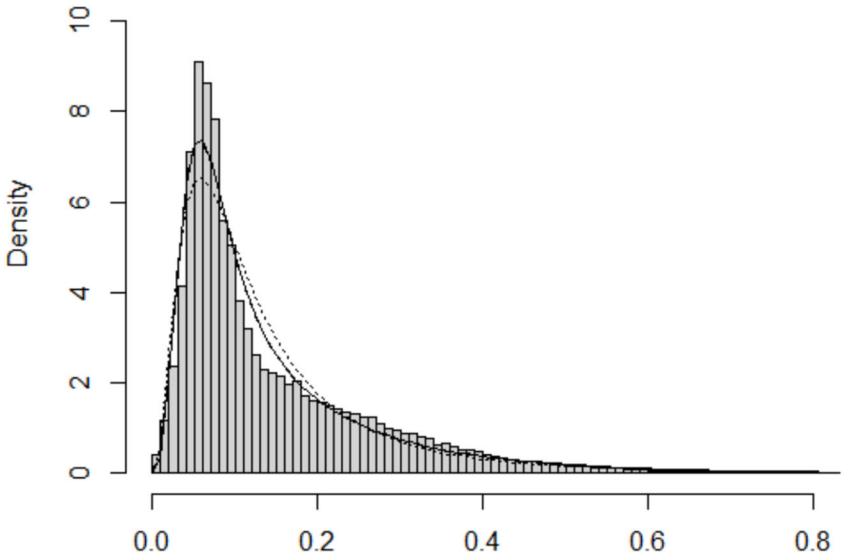

Fig. 7 Histogram of the diffused irradiance index (UP) data with the three best-fitted PDFs. The BP-NB (dashed line), LN-LN (dotted line), G-NB (solid line)

and BIC support the G-NB as the best fit (indicated in bold), followed by the BP-NB for both locations. It is observed that the Poisson mixing distribution for these datasets is not a good choice.

4.1.2 Norwegian fire claims

This dataset contains 9181 fire insurance claims, in thousands of Norwegian krones (NKR), for a Norwegian insurance company from 1972 − 1992. This dataset is available in the `R` package `Reins`. The data were recorded with a priority of 500 thousand NKR, and thus, 500 thousand was deducted from each observation to ensure the positivity of the data. Numerous authors studied this dataset; see for example [37], [7], [8], and [5]. As in previous investigations, the same top-performing models from the paper [37], were applied and considered. Figure 9 and Table 4 report that the AIC and BIC provide the same ranking with the best model (indicated in bold), the G-G, followed by the G-NB.

5 Conclusion

We propose a discrete mode-mixture (DMM) where the unimodal mode-parameterized distribution is the conditional model (basic component or reference distribution) and a discrete

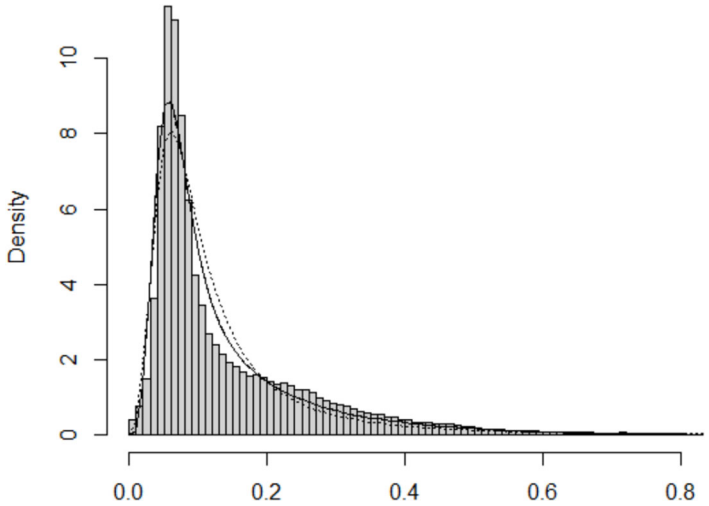

Fig. 8 Histogram of the diffused irradiance index (SUN) data with the three best-fitted PDFs. The BP-NB (dashed line), LN-LN (dotted line), G-NB (solid line)

Table 2 Diffused irradiance index (UP) data: log-likelihood, AIC, and BIC for the competing models, along with rankings based on these criteria

Model	#par	Log-lik	AIC	Ranking	BIC	Ranking
Gamma (G)	2	201373.6	402743.1	8	402722.6	8
G-P	3	201373.6	402741.1	9	402710.4	9
G-NB	4	215571.9	**431135.9**	1	**431094.9**	1
Beta Prime (BP)	2	205416.1	410828.3	6	410807.8	5
BP-P	3	205416.1	410826.3	7	410795.5	6
BP-NB	4	215381.5	430755.0	2	430714.0	2
LN-LN	3	211989.9	423973.9	4	423943.1	3
G-G	3	208945.6	417885.2	5	417866.7	4
IG-IG	3	204604.9	423974.9	3	409185.3	7

Table 3 Diffused irradiance index (SUN) data: log-likelihood, AIC, and BIC for the competing models, along with rankings based on these criteria

Model	#par	Log-lik	AIC	Ranking	BIC	Ranking
Gamma (G)	2	193631.5	387259.0	8	387238.6	8
G-P	3	193631.5	387257.0	9	387226.5	9
G-NB	4	214584.9	**429161.8**	1	**429121.2**	1
Beta Prime (BP)	2	197707.9	395411.8	6	395391.5	6
BP-P	3	197707.9	395409.8	7	395379.3	7
BP-NB	4	214297.6	428587.2	2	428546.6	2
LN-LN	3	208644.6	417283.2	3	417252.7	3
G-G	3	204766.1	409526.2	4	409495.7	4
IG-IG	3	204490.5	408975.0	5	408969.8	5

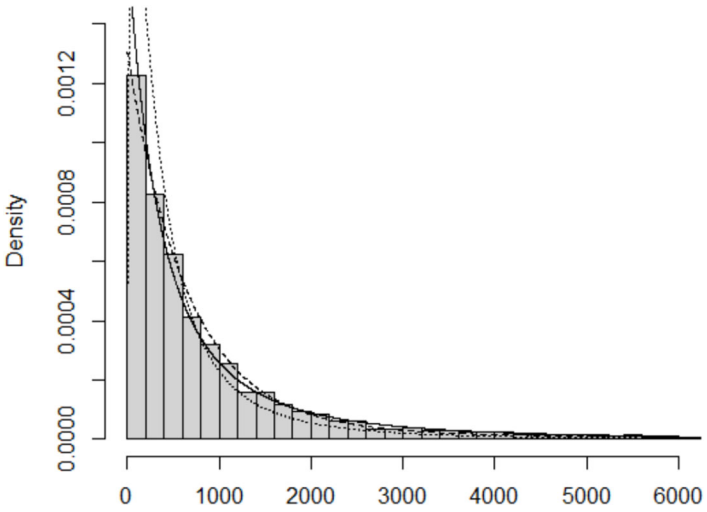

Fig. 9 Histogram of the Norwegian fire claims data with the three best-fitted PDFs. The G-NB (dashed line), BP-NB (dotted line), Gamma-gamma (solid line).

Table 4 Norwegian fire claims data: log-likelihood, AIC, and BIC for the competing models, along with rankings based on these criteria

Model	#par	Log-lik	AIC	Ranking	BIC	Ranking
Gamma (G)	2	−77565.3	−155134.7	5	−155148.9	5
G-P	3	−77565.3	−155136.7	6	−155158.0	6
G-NB	4	−73952.3	−147912.6	2	−147941.1	2
Beta Prime (BP)	2	−162861.9	−325727.9	8	−325742.1	8
BP-P	3	−107823.6	−215653.1	7	−215674.5	7
BP-NB	4	−74964.3	−149936.6	3	−149965.1	3
LN-LN	3	−75333.5	−150672.9	4	−150694.3	4
G-G	2	−73857.6	**−147721.2**	1	**−147742.5**	1

mixing variable superimposed on the mode of the basic component, and obtain closed-form expressions for the pdfs. However, the novelty of this approach is not limited to these models. The introduced models were applied to two real datasets, and upon calculating the information criteria, including AIC and BIC, the new models yielded the most favorable results in both cases. A model that suits a particular data set may not exclusively outperform other candidates of the same kind; thus, this paper is not to claim better modeling but to introduce a new formulation and thought direction, focusing on the mode. The uniqueness of the focus on the location of the mode gives the practitioner the leverage for informed insight detection. Our results yield the basis for future research with the mode mixture as the focus, for example, in a multivariate setting.

6 Mode(s) of considered DMM models

To establish the unimodality of the models (5) and (6), consider the following outline, choosing the Poisson (7) as mixing distribution. From (5) the mode $m_{\text{G-P}}$ of the G-P can be determined from the derivative of (5) set to 0:

$$\sum_{j=0}^{\infty} \frac{\left(\frac{\lambda}{2}\right)^j}{j!\Gamma\left(\frac{\theta}{\gamma}+j+1\right)\gamma^{\frac{\theta}{\gamma}+j+1}} \left\{\exp\left(-\frac{x}{\gamma}\right) x^{\frac{\theta}{\gamma}+j-1}\left[-\frac{x}{\gamma}+\frac{\theta}{\gamma}+j\right]\right\}$$

which implies that

$$\sum_{j=0}^{\infty} \frac{\left(\frac{\lambda}{2}\right)^j}{j!\Gamma\left(\frac{\theta}{\gamma}+j+1\right)\gamma^{\frac{\theta}{\gamma}+j+1}} \left\{-\frac{x}{\gamma}+\frac{\theta}{\gamma}+j\right\} = 0.$$

After some simplification, it follows

$$m_{\text{G-P}} = \theta + \gamma \frac{\Gamma\left(\frac{\theta}{\gamma}+1\right)}{{}_0F_1\left(\frac{\theta}{\gamma}+1;\frac{\lambda}{2\gamma}\right)} \sum_{j=1}^{\infty} \frac{\left(\frac{\lambda}{2\gamma}\right)^j}{\Gamma(j)\,\Gamma\left(\frac{\theta}{\gamma}+j+1\right)}.$$

In all of the respective cases, it is clear that the respective modes from the DMM distributions considered in this paper are larger than, or equal to, the true conditional mode θ. In addition, when $\lambda \to 0$ and $r \to 1$, the nested conditional mode θ is obtained.

Acknowledgements This work was based upon research supported in part by the National Research Foundation (NRF) of South Africa (SA), grant RA201125576565, nr 145681; NRF ref. SRUG2204203965; UID 119109; the Department of Research and Innovation at the University of Pretoria (SA), the Faculty of Science at the University of the Witwatersrand, as well as the DSI-NRF Centre of Excellence in Mathematical and Statistical Sciences (CoE-MaSS). The opinions expressed and conclusions arrived at are those of the authors and are not necessarily to be attributed to the NRF.

Funding Open access funding provided by University of Pretoria.

References

1. Akaike, H.: A new look at the statistical model identification. IEEE Trans. Autom. Control **19**, 716–723 (1974)
2. Andrews, D.F., Mallows, C.L.: Scale mixtures of normal distributions. J. Roy. Stat. Soc.: Ser. B (Methodol.) **36**, 99–102 (1974)
3. Assuncao, H., Escobedo, J., Oliveira, A.: Modelling frequency distributions of 5 minute-averaged solar radiation indexes using beta probability functions. Theoret. Appl. Climatol. **75**, 213–224 (2003)
4. Bagnato, L., Punzo, A.: Finite mixtures of unimodal beta and gamma densities and the k-bumps algorithm. Comput. Statistics **28**, 1571–1597 (2013)
5. Bakar, S.A., Nadarajah, S., Ngataman, N.: A family of density-hazard distributions for insurance losses. Commun Statistics-Simulation Comput **51**, 5857–5875 (2022)

6. Bekker, A., Ferreira, J.: Bivariate gamma type distributions for modeling wireless performance metrics. Stat. Optim. & Inf. Comput. **6**, 335–353 (2018)
7. Benatmane, C., Zeghdoudi, H., Shanker, R., Lazri, N.: Composite Rayleigh-Pareto distribution: Application to real fire insurance losses data set. J. Stat. Manag. Syst. **24**, 545–557 (2021)
8. Brazauskas, V., Kleefeld, A.: Modeling severity and measuring tail risk of Norwegian fire claims. North American Actuarial J. **20**, 1–16 (2016)
9. Chacón, J.E.: The modal age of statistics. Int. Stat. Rev. **88**, 122–141 (2020)
10. Chen, S.X.: Probability density function estimation using gamma kernels. Ann. Inst. Stat. Math. **52**, 471–480 (2000)
11. Dubey, S.D.: Compound gamma, beta and F distributions. Metrika **16**, 27–31 (1970)
12. Erdelyi, A., Magnus, W., Oberhettinger, F., Tricomi, F.G.: Tables of Integral Transforms: Vol. 1, McGraw-Hill Book Company, Incorporated (1954)
13. Ferreira, J., Bekker, A., Arashi, M.: Bivariate noncentral distributions: an approach via the compounding method. S. Afr. Stat. J. **50**, 103–122 (2016)
14. Ferreira, J., van der Merwe, A.: A noncentral Lindley construction illustrated in an INAR(1) environment. Stats **5**, 70–88 (2022)
15. Gerstenkorn, T.: A compound of the generalized negative binomial distribution with the generalized beta distribution. Open Mathematics **2**, 527–537 (2004)
16. Gradshteyn, I.S., Ryzhik, I.M.: Table of integrals, series, and products. Academic Press (2014)
17. Greenwood, M., Yule, G.U.: An inquiry into the nature of frequency distributions representative of multiple happenings with particular reference to the occurrence of multiple attacks of disease or of repeated accidents. J. Roy. Stat. Soc. **83**, 255–279 (1920)
18. Gurland, J.: Some interrelations among compound and generalized distributions. Biometrika **44**, 265–268 (1957)
19. Jones, M.: Generating distributions by transformation of scale. Stat. Sin. **24**, 749–771 (2014)
20. Jones, M.: On families of distributions with shape parameters. Int. Stat. Rev. **83**, 175–192 (2015)
21. Kim, J., Mahmassani, H.S.: Compound gamma representation for modeling travel time variability in a traffic network. Transportation Research Part B: Methodological **80**, 40–63 (2015)
22. Kruschke, J.: Doing Bayesian Data Anal: A Tutorial With R, JAGS, and Stan. Academic Press (2014)
23. Lohmann, G.M., Hammer, A., Monahan, A.H., Schmidt, T., Heinemann, D.: Simulating clear-sky index increment correlations under mixed sky conditions using a fractal cloud model. Sol. Energy **150**, 255–264 (2017)
24. Mathai, A.M., et al.: A handbook of generalized special functions for statistical and physical sciences. Oxford University Press, USA (1993)
25. Mazza, A., Punzo, A.: Modeling household income with contaminated unimodal distributions. In: Petrucci, A., Racioppi, F., Verde, R. (eds.) New Statistical Developments in Data Science, pp. 373–391. Springer, Cham, Switzerland (2019)
26. Munkhammar, J., Widén, J.: An autocorrelation-based copula model for producing realistic clear-sky index and photovoltaic power generation time-series, In: 2017 IEEE 44th Photovoltaic Specialist Conference (PVSC), IEEE. pp. 3067–3072 (2017)
27. Mutavhatsindi, T., Sigauke, C., Mbuvha, R.: Forecasting hourly global horizontal solar irradiance in South Africa using machine learning models. IEEE Access **8**, 198872–198885 (2020)
28. Nascimento, A., Rêgo, L.C., Silva, J.W.: Compound truncated Poisson gamma distribution for understanding multimodal SAR intensities. J. Applied Stat, 1–20 (2022)
29. Nations, U.: Transforming our world: the 2030 agenda for sustainable development. Technical Report. New York. https://sustainabledevelopment.un.org/topics (2015)
30. Negarestani, H., Jamalizadeh, A., Shafiei, S., Balakrishnan, N.: Mean mixtures of normal distributions: properties, inference and application. Metrika **82**, 501–528 (2019)
31. Otto, A., Ferreira, J., Bekker, A., Punzo, A., Tomarchio, S.: A refreshing take on the inverted Dirichlet via a mode parameterization with some statistical illustrations. Journal of the Korean Statistical Society **54**, 314–341 (2025)
32. Panjer, H.H., Willmot, G.E.: Compound Poisson models in actuarial risk theory. J. Econ. **23**, 63–76 (1983)
33. Pasari, S., Nandigama, V.S.S.K.: Statistical modeling of solar energy. In: Enhancing Future Skills and Entrepreneurship, pp. 157–165. Springer, Cham (2020)
34. Patnaik, P.: The non-central χ 2-and F-distribution and their applications. Biometrika **36**, 202–232 (1949)
35. Prak, D., Teunter, R., Babai, M.Z., Boylan, J.E., Syntetos, A.: Robust compound Poisson parameter estimation for inventory control. Omega **104**, 102481 (2021)
36. Punzo, A.: A new look at the inverse Gaussian distribution with applications to insurance and economic data. J. Appl. Stat. **46**, 1260–1287 (2019)

37. Punzo, A., Bagnato, L., Maruotti, A.: Compound unimodal distributions for insurance losses. Insurance Math. Econom. **81**, 95–107 (2018)
38. Punzo, A., Mazza, A., Maruotti, A.: Fitting insurance and economic data with outliers: a flexible approach based on finite mixtures of contaminated gamma distributions. J. Appl. Stat. **45**, 2563–2584 (2018)
39. R Core Team: R: A Language and Environment for Statistical Computing. R Foundation for Statistical Computing. Vienna, Austria. https://www.R-project.org/ (2022)
40. Schwarz, G.: Estimating the dimension of a model. The Annal Stat., 461–464 (1978)
41. Shevchenko, P.: Calculation of aggregate loss distributions. ArXiv preprint arXiv:1008.1108 (2010)
42. Tomarchio, S.D., Punzo, A.: Dichotomous unimodal compound models: application to the distribution of insurance losses. J. Appl. Stat. **47**, 2328–2353 (2020)
43. Tomarchio, S.D., Punzo, A., Ferreira, J.T., Bekker, A.: Mode mixture of unimodal distributions for insurance loss data. Annals of Operations Research , 1–19 (2024)
44. Tovar-Pescador, J. Modelling the statistical properties of solar radiation and proposal of a technique based on Boltzmann statistics, In: Modeling Solar Radiation at the Earth's Surface. Springer, pp. 55–91 (2008)
45. Twala, S., Ye, X., Xia, X., Zhang, L.: Optimal integration of solar home systems and appliance scheduling for residential homes under severe national load shedding. J. Autom Intell **2**, 227–238 (2023)
46. du Venage, G.: South Africa comes to standstill with Eskom's load shedding. Eng. Min. J. **221**, 18–18 (2020)
47. Wagener, M., Bekker, A., Arashi, M.: Mastering the body and tail shape of a distribution. Math. **9**, 2648 (2021)
48. Wang, Z.: One mixed negative binomial distribution with application. J. Stat Planning and Inference **141**, 1153–1160 (2011)
49. West, M.: On scale mixtures of normal distributions. Bio. **74**, 646–648 (1987)
50. Withers, C., Nadarajah, S.: On the compound Poisson-gamma distribution. Kybernetika **47**, 15–37 (2011)
51. Yunus, R.M., Khan, S.: The bivariate noncentral chi-square distribution-a compound distribution approach. Appl. Math. Comput. **217**, 6237–6247 (2011)